Case Studies in Chemical and Environmental Engineering 9 (2024) 100703

Contents lists available at ScienceDirect

Case Studies in Chemical and Environmental Engineering

journal homepage: www.sciencedirect.com/journal/case-studies-in-chemical-and-environmental-engineering

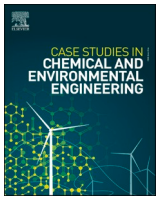

Case Report

Assessment of atmospheric corrosivity in coastal zones: Case study in port Lopez, Manabí, Ecuador

Juan Carlos Guerra-Mera [a], Ángel Ramón Sabando García [b], Miriam Goretty Pin -Mera [c], Joan Manuel Rodríguez-Díaz [d,e,*], Abel Castañeda-Valdés [f,**]

[a] Departamento de Construcciones Civiles, Facultad Ingeniería y Ciencias Aplicadas. Universidad Técnica de Manabí (UTM), Avenida Urbina, Portoviejo, 130105, Ecuador
[b] Pontificia Universidad Católica Del Ecuador Sede Santo Domingo, Santo Domingo, CP 230203, Santo Domingo de los Tsáchilas, Ecuador
[c] Unidad Educativa 25 de Mayo, Crucita, Manabí, Ecuador
[d] Laboratorio de Análisis Químicos y Biotecnológicos. Instituto de Investigación, Universidad Técnica de Manabí, Av. Urbina y Che Guevara, Portoviejo, Manabí, Ecuador
[e] Departamento de Procesos Químicos, Facultad Ingeniería y Ciencias Aplicadas. Universidad Técnica de Manabí (UTM), Avenida Urbina, Portoviejo, 130105, Ecuador
[f] Laboratorio de Corrosión y Protección de Materiales. Dirección de Investigación, Desarrollo e Innovación. Centro Nacional de Investigaciones Cientfficas CNIC, Avenida 25 Y 158, Playa, 11600, La Habana, Cuba

ARTICLE INFO

Keywords:
Corrosivity categories
Chloride deposition
Humidity
Oxygen's solubility
Coastal environment

ABSTRACT

This manuscript investigates the atmospheric corrosion of carbon steel in Puerto Lopez, a coastal region in Manabí Province, Ecuador. For the study, six outdoor exposure sites (OES) were strategically placed at different distances from the coast to evaluate the impact of meteorological factors on the chloride deposition rate ($Cl^{-}DR$) and how proximity to the coast could influence atmospheric corrosivity to carbon steel. It identified a critical threshold for the monthly average wind speed that escalates $Cl^{-}DR$, noted as one of the lowest globally. The findings revealed a medium corrosivity category (C3) for carbon steel in the inland OES, suggesting the significant role of high relative humidity (RH) typical of the area in possibly reducing $Cl^{-}DR$ through saline dissolution. Moreover, the interaction between high RH and $Cl^{-}DR$ could markedly diminish oxygen's solubility in water collected in oxide layer interstices and on the carbon steel surfaces, potentially affecting the cathodic oxygen reaction. Nonetheless, the study confirms the continuing influence of $Cl^{-}DR$ on the atmospheric corrosion of carbon steel. Predictive corrosivity categories for carbon steel in this coastal environment span from two to twenty years across the OES, underlining the critical need for understanding and mitigating corrosion in similar settings.

1. Introduction

Coastal zones in Ecuador, like those in many South American countries, are recognized for their high construction potential, particularly due to the burgeoning tourism industry. Major industries, including thermoelectric plants and refineries, often utilize seawater in their cooling systems and are strategically located near coastlines or bay areas. Consequently, conducting atmospheric corrosion studies is imperative prior to initiating construction, maintenance, or rehabilitation projects [1,2]. Incorporating the results of these studies into the design phase is crucial for selecting appropriate materials—be it metallic, inorganic, organic, or composite—and their primary and secondary protection systems, which are typically coating-based. Carbon steel, known for its high mechanical strength, is a predominant choice for infrastructure construction. Conversely, reinforced concrete, the most prevalent composite material in the construction sector, suffers significant deterioration in coastal zones due to atmospheric corrosion of the steel reinforcement [3,4].

A regulatory framework for compensating atmospheric corrosion impacts on electric power transmission infrastructure has been established in Colombia, alongside mathematical models to represent atmospheric corrosion, material degradation, and their effects on

* Corresponding author. Laboratorio de Análisis Químicos y Biotecnológicos. Instituto de Investigación, Universidad Técnica de Manabí, Av. Urbina y Che Guevara, Portoviejo, Manabí, Ecuador.
** Corresponding author.
E-mail addresses: juan.guerra@utm.edu.ec (J.C. Guerra-Mera), arsabando@pucesd.edu.ec (Á.R.S. García), mipime73@hotmail.com (M.G. Pin -Mera), joan.rodriguez@utm.edu.ec (J.M. Rodríguez-Díaz), abel.castaneda@cnic.cu (A. Castañeda-Valdés).

https://doi.org/10.1016/j.cscee.2024.100703
Received 27 February 2024; Received in revised form 21 March 2024; Accepted 22 March 2024
Available online 23 March 2024

infrastructure's technical and service life. According to specialty standards on atmospheric corrosion issued since 2012, the corrosivity categories determined for commonly used building materials (primarily carbon steel, zinc, copper, and aluminum) can also be applied to other materials [5]. Research in tropical coastal climates, such as Cuba's, has shown that high to extreme corrosivity categories have led to severe deterioration of inorganic materials like bricks and elastomeric polymers, along with significant cracking in concrete due to reinforcement steel corrosion [6–8].

Historically, Ecuador has seen limited atmospheric corrosion studies, with only seven outdoor exposure sites (OES) established across the country in the last century, four of which were in high-potential coastal zones [9]. More recently, eight additional OES were established, seven in Quito and one in the coastal city of Esmeraldas [10]. Despite Quito's urban location, its construction potential is notable, especially with air pollution from local refineries and thermoelectric plants elevating the atmospheric corrosivity for building materials. However, the marine influence was minimal due to the sites' locations, indicating a potential risk for intense deterioration in metallic and concrete structures [11].

Since 2016, Manabí province, with its extensive coastline and significant tourism potential, has become a focal point for atmospheric corrosion studies on carbon steel. Prior to this, no studies had been conducted in the province either in the last century or the first fifteen years of the current one. In total, 51 OES have been installed across various cantons, with findings from the first three cantons already published [12,13].

This study aims to evaluate the atmospheric corrosivity categories for carbon steel in Port Lopez's coastal zone over one year. It distinguishes itself from previous studies by offering a detailed description of the aggressive coastal atmospheric environment and predicting corrosivity categories for exposure times extending beyond one year, ranging from two to twenty years.

2. Experimental section

This study was conducted in Port Lopez, a coastal city in Ecuador and the cantonal capital of the Port Lopez Canton, ranking as the eleventh most populous city in the Manabí Province. The geographical coordinates for the study area are 1°33′32″S, 80°48′38″W.

2.1. Outdoor exposure sites

Six outdoor exposure sites (OES) were established at varying distances from the coastline (OES-2 = 20 m, OES-3 = 100 m, OES-4 = 250 m, OES-5 = 600 m, OES-6 = 930 m, OES-7 = 1000 m). Uniquely, one site (OES-1 = −100 m) was positioned beyond the wave breaker zone, extending into the sea, which differs from the placement strategies in other coastal zones of Manabí and global studies.

At each OES, the following were installed on wooden racks.

- Three dry cloth devices (150 × 100 mm) to measure the chloride deposition rate.
- Six carbon steel samples (75 × 50 mm) to assess the atmospheric corrosion rate.

To minimize the impact of rain and thus prevent washing effects, these racks were sheltered and mounted at a height of 3 m above the ground. They were inclined at a 45° angle facing west-northwest (WNW), the direction from which the prevailing winds blow.

2.2. Meteorological parameters

The study analyzed monthly average values for key meteorological parameters: Relative Humidity (*RH-%*), Temperature (T-°C), and Wind Speed (*V-m/s*), which were recorded from December 2016 to November 2017. These data were sourced from the Cantagallo Meteorological Station, a facility endorsed by the National Institute of Meteorology and Hydrology of Ecuador, situated in proximity to the research area. Specifically, the average wind speed values were measured in alignment with the predominant wind direction, which is west-northwest (WNW). In accordance with atmospheric corrosion standards, when direct measurements of the *HR-T-V* complex are not feasible due to a lack of specialized equipment or devices, utilizing data from the nearest meteorological service to the study area is an acceptable practice [14].

2.3. Measurement of chloride deposition rate

In accordance with atmospheric corrosion standards, absorbent cloth pieces of size 150 mm × 100 mm were used as dry cloth device to determine chloride deposition rate ($Cl^{-}DR$-mg $m^{-2}d^{-1}$) [15]. Preparation: Three dry plate devices were perfectly cleaned, washed with distilled water and dried before exposing them on each OES. Dry plate devices were exposed monthly during one year. Before placement and after monthly collection from each OES, the dry cloth devices were preserved in desiccators to prevent any alterations. The chemical-analytical method utilized for the monthly determination of $Cl^{-}DR$ was volumetric titration [15]. The chloride deposition rate ($Cl^{-}DR$-mg $m^{-2}d^{-1}$) was determined monthly throughout the study period (December 2016 to November 2017) for each OES. Three measurements were taken per dry cloth device each month at every OES. Given the similarity among the three measurements, their average was calculated and reported on a monthly basis. Additionally, the overall average and standard deviations for each OES were derived from these monthly averages and depicted in the analysis. Furthermore, the annual average $Cl^{-}DR$ values were illustrated as a function of distance from the coastline (d, in meters), adopting a model based on a decreasing exponential function:

$$Cl^{-}DR = Cl^{-}DR_{m} + ae^{-d/t} \quad (1)$$

$Cl^{-}DR_{m}$ represents the vertical asymptote or the theoretical annual average $Cl^{-}DR$ value observable from the closest monitoring OES up to a considerable distance inland; a statistical coefficient, t critical distance from the coastline where the $Cl^{-}DR_{m}$ remains constant into the interior of the earth.

2.3.1. Influence of meteorological parameters on $Cl^{-}DR$

To demonstrate the influence of meteorological parameters (*RH*, *T*, *and V*) on $Cl^{-}DR$, it was necessary to fit a statistical model for each OES based on multiple regressions:

$$Cl^{-}DR = m \pm b[RH] \pm c[T] \pm d[V] \quad (2)$$

The 12 monthly average values of $Cl^{-}DR$ calculated in each OES, were taken as the dependent variable. The 12 monthly average values of *RH, T,* and *V* were taken as the independent.

On the other hand, to demonstrate the critical threshold of *V* at which $Cl^{-}DR$ increased, another model based on an increasing exponential function was fitted:

$$Cl^{-}DR = ne^{V/t} \quad (3)$$

The 12 annual average values of $Cl^{-}DR$ calculated, were taken as the dependent variable. The 12 monthly average values of *V* were taken as the independent. A data of n = 12 was established for both fits (2), and (3).

2.4. Measurement of atmospheric corrosion rate

In accordance with atmospheric corrosion standards, carbon steel samples (75 × 50 mm) were used to assess the atmospheric corrosion rate [16]. The atmospheric corrosion rate (r_{corr}-$g\ m^{-2}$) was quantified monthly for each Outdoor Exposure Site (OES) throughout the study period (December 2016 to November 2017). For each OES, three

values—one per carbon steel specimen—were obtained monthly. Due to the consistency among these measurements, the average monthly corrosion rates were calculated for each site and graphically represented.

To ascertain the corrosivity categories of the atmosphere for carbon steel at each OES within the study area, annual atmospheric corrosion rates (r_{corr}-$g\ m^{-2}y$ *and* $\mu m/y$) were computed from the three remaining carbon steel specimens that were exposed throughout the year.

Preparation of the carbon steel specimens involved degreasing, pickling, and initial weighing (in grams) 24 hours before their placement at each OES [16]. The atmospheric corrosion rate for the carbon steel specimens was calculated using the gravimetric method (r_{corr}-$g\ m^{-2}y$). This method involves calculating the difference between the initial and final weights, normalized over the exposure area (m^2) and the duration of exposure ($y = 1\ year$), facilitating the determination of the corrosion rate [17]. From the quotient between annual atmospheric corrosion rates (r_{corr}-$g\ m^{-2}y$) calculated and carbon steel density (7.86 g m^{-3}), annual atmospheric corrosion rates (r_{corr}-$\mu m\ y^{-1}$) were determined.

2.5. Influential factors onthe monthly atmospheric corrosion rate

To demonstrate the most influential factors on the monthly atmospheric corrosion rate of carbon steel, statistical model based on multiple regressions were fitted in each OES:

$$r_{corr} = p + b[Cl^{-}DR] \pm c[RH] \pm d[T] \pm e[V] \quad (4)$$

The monthly average values of atmospheric corrosion rate in the carbon steel specimens from the 12 calculated values in the three specimens in each OES were taken as the dependent variable (r_{corr}). The monthly average values of the meteorological parameters *RH, T*,*V* and $Cl^{-}DR$ were taken as the independent variables. A data of n = 12 was established.

2.6. Prediction of the corrosivity categories of the atmosphere

To predict the corrosivity categories of the atmosphere for carbon steel at times of exposure longer than one year (from two to 20 years) in each OES, the statistical model established in the atmospheric corrosion specialty standard was used [18]:

$$D = r_c t^b \quad (5)$$

Where:

D: atmospheric corrosion predicted on the metallic material ($g\ m^{-2}$) over the time of exposure.

r_c: Annual atmospheric corrosion rate experimentally determined at the year of study ($g\ m^{-2}$ and μm). In this case annual average values of atmospheric corrosion rate calculated from each OES were used.

t: time of exposure (years).

*b:*exponent specifying the interaction between the metallic material and the atmosphere selected in the atmospheric corrosion specialty standard for each exposure time (from 2 to 20 years).

3. Results and discussion

3.1. Characterization of the aggressive coastal atmospheric environment

3.1.1. Meteorological parameters' monthly averages

The study revealed distinct seasonal variations in meteorological parameters within the coastal zone. From June to November, the region exhibited higher Relative Humidity (*RH*) and lower temperatures (*T*), as depicted in Fig. 1. This contrasts with patterns observed in other studies across coastal zones in Manabí, between Bahía de Caráquez-San Vicente and Manta port areas, where higher *RH* and *T* averages were noted during the December–May period, coinciding with the rainiest months

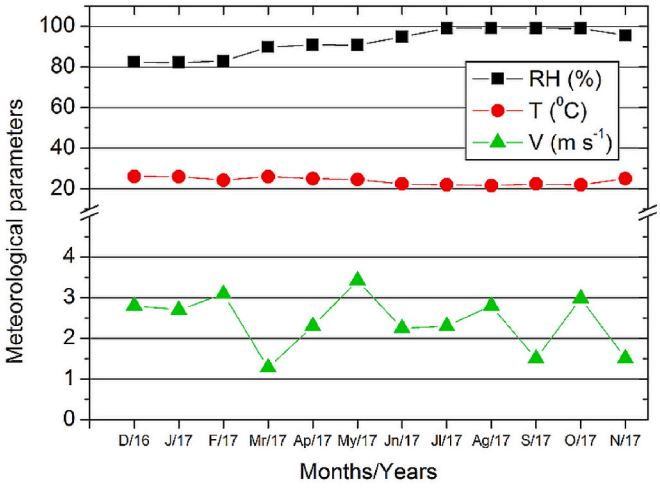

Fig. 1. Behavior of the monthly average values of the *RH-T*, and *V* in the study zone.

in Ecuador's coastal climates.

Such discrepancies suggest the potential presence of a unique microclimate within the study area, which could significantly influence the atmospheric corrosivity, especially concerning carbon steel. This period's atmospheric conditions, categorized from high (C4) to extreme (CX) corrosivity levels at proximities close to the shoreline, underscore the aggressive nature of this coastal environment.

Annual averages of the *RH-T* complex were recorded at 92% and 24 °C, respectively, indicating that chloride deposition occurs in saline solution rather than crystallizing as dry salts. Similar conditions have been observed in coastal zones of high construction potential in countries like Cuba and Brazil [19,20], where such environments significantly contribute to the high corrosivity categories for metal and reinforced concrete structures.

Moreover, the study highlighted a variable trend in wind speed (*V*) across different months, a factor less frequently analyzed in conjunction with *RH* and *T* in atmospheric corrosion studies. Unlike the referenced research in Manabí's high construction potential coastal zones and tropical climates of Cuba, higher wind speeds were noted during the less rainy seasons—winter in Cuba and summer in Ecuador. This distinction further supports the hypothesis of a unique microclimate within the study zone, emphasizing the complex interplay of meteorological parameters in determining atmospheric corrosivity levels against carbon steel and potentially other materials [21,22].

3.1.2. Chloride deposition rate ($Cl^{-}DR$) monthly averages

The chloride deposition rate ($Cl^{-}DR$) displayed significant variability throughout the study, with notable peaks during both the rainy (December–May) and dry (June–November) seasons, as well as in months experiencing higher average wind speeds (V), as illustrated in Fig. 2 a and b.

This variability suggests a complex interaction between $Cl^{-}DR$ and various factors, including distance from the coastline and meteorological parameters, particularly wind speed. The $Cl^{-}DR$ exhibited a decreasing trend with increasing distance from the shoreline (Fig. 2a), highlighting the direct influence of proximity to the sea and wind dynamics on chloride deposition rates.

Comparative analysis with previous studies in coastal zones of Manabí, such as Bahía de Caráquez-San Vicente and Manta port areas, revealed higher $Cl^{-}DR$ values during their rainiest winter seasons. Conversely, in Cuba, elevated $Cl^{-}DR$ values were observed during the dry winter season, leading to the identification of high (C4), very high (C5), and extreme (CX) atmospheric corrosivity categories for carbon steel. These findings were facilitated by the use of dry cloth devices for

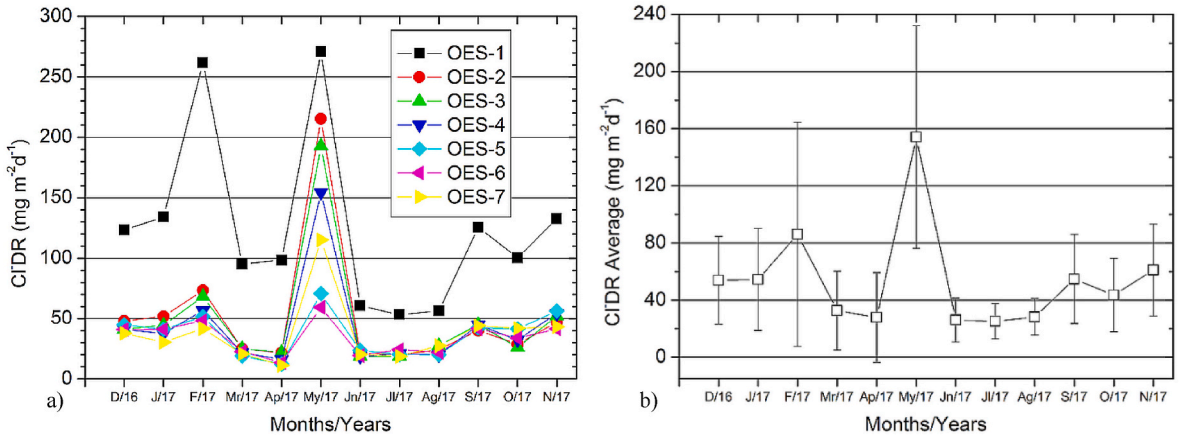

Fig. 2. Behavior of monthly average values of $Cl^{-}DR$ a), and the average values b).

determining $Cl^{-}DR$, underscoring the methodological consistency across different geographic studies [23,24].

The pronounced variability in $Cl^{-}DR$ further substantiates the hypothesis of a unique microclimate within the study area. It is noteworthy that atmospheric corrosion studies often reveal seasonal $Cl^{-}DR$ peaks, which are influenced by the specific climatic conditions of the study location.

Moreover, this research aligns with other studies conducted in Manabí, including the coastal zone of Port Lopez, in highlighting $Cl^{-}DR$'s high variability. Such variability is especially pronounced where higher monthly and average $Cl^{-}DR$ values were recorded (Fig. 2b), emphasizing the dynamic and complex nature of chloride deposition in coastal environments.

3.1.3. Impact of coastal distance on chloride deposition rate ($Cl^{-}DR$)

The influence of distance from the coastline on the chloride deposition rate ($Cl^{-}DR$) is significant, with a clear decrease in $Cl^{-}DR$ values as the distance increases, as evidenced by annual average $Cl^{-}DR$ values (Fig. 3). This trend is well-represented by the fitted model (1), indicating a strong correlation between $Cl^{-}DR$ and coastal proximity. The model's $Cl^{-}DR\_m$ value, which stands at 38.33, represents the vertical asymptote or the theoretical annual average $Cl^{-}DR$ value observable from the closest monitoring site (OES-2 = 20 m) up to a considerable distance inland (OES-7 = 1000 m). This suggests a persistently high $Cl^{-}DR$, and consequently, a higher corrosivity risk for carbon steel within this range.

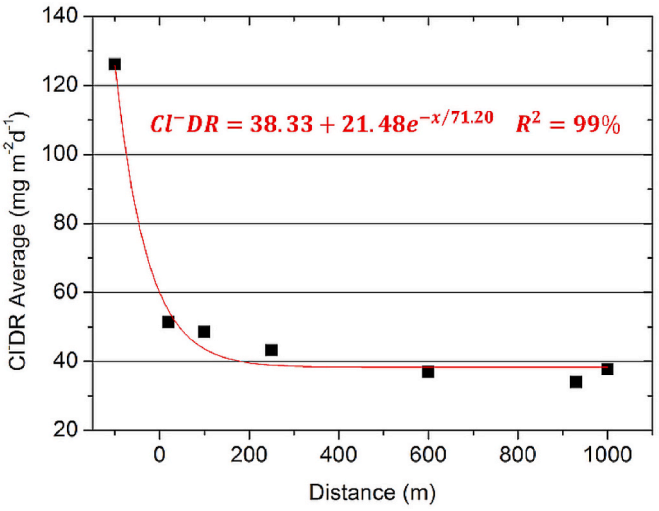

Fig. 3. Annual average values decrease with the distance from the coastline increased.

According to the value of t shown in the fitted model, from a distance of 70 m from the coastline, a considerable decrease of the $Cl^{-}DR$ is possible (Fig. 3).

Internationally, this phenomenon has been substantiated through various studies in coastal regions, employing different statistical models and devices for $Cl^{-}DR$ measurement. These models consistently confirm the decrease in $Cl^{-}DR$ with increased distance from the shoreline, highlighting a global pattern of atmospheric corrosion dynamics influenced by marine environments.

For instance, research in the Mediterranean coast of Spain and the Pacific coast of Manta in Ecuador (Table 1) utilized similar models, identifying high atmospheric corrosivity categories for carbon steel up to approximately 1 km from the coast. These findings align with other studies from diverse coastal contexts, such as Brazil, Cuba, Sweden, South Korea, and Australia, each adopting unique methodologies for $Cl^{-}DR$ assessment, ranging from dry plates and wet candles to sophisticated salinity measurement devices.

Interestingly, in Cuba and Brazil, a distinct drop in $Cl^{-}DR$ was observed just a short distance from the coastline, attributed to the shielding effect of reinforced concrete structures which intercept up to 90% of chloride ion salts within 30 m of the shoreline (t = 30). This phenomenon led to the identification of an atmospheric corrosivity category exceeding extreme (>CX) levels for carbon steel in certain Cuban studies [33].

Conversely, the presence of an estuary between Bahía de Caráquez and San Vicente in Ecuador introduced an anomalous $Cl^{-}DR$ pattern, deviating from the expected decrease with distance. This exception was captured through polynomial regression models, underscoring the unique aggressiveness of this environment towards carbon steel. Such variability emphasizes the complexity of atmospheric corrosion processes and the significant influence of local geographical and meteorological conditions on $Cl^{-}DR$.

3.1.4. Analysis of meteorological parameters on chloride deposition rate ($Cl^{-}DR$)

Limited research has been conducted on the effects of meteorological parameters (RH, T and V) on $Cl^{-}DR$. Nonetheless, preliminary findings from studies in coastal regions with significant construction potential in Cuba and Manabí, Ecuador, offer insightful observations. Notably, an increase in RH significantly affects $Cl^{-}DR$, as evidenced by the application of model (2) across various OES, along with the collective model average presented (Table 2). However T and V, were not determinants in the derived models.

Due to m values were negative in the regressions fitted, high values of RH correlates a decrease in $Cl^{-}DR$ in a saline solution. $Cl^{-}DR$ values were negatives (Table 2).

By comparing the experimental correlation coefficients (r_{exp}) with

Table 1
Different studies carried out in coastal zones around the world.

References	Country	Models	Environment	Devices
[12]	Ecuador	$Cl^{-}DR = a \pm b(D) \pm c(D)^2$	CoastalzonebetweenthecantonsBahía de Caráquez- San Vicente. Pacific Ocean	Dry Plate
[13]		$Cl^{-}DR = Cl^{-}DR_m + ae^{-d/t}$	Coastal zone of the canton of Manta. Pacific Ocean	
[25]	Spain	$Cl^{-}DR = Cl^{-}DR_m + ae^{-d/t}$	Coastal zone of Mediterranean Spanish	Wet candle
[26]	Brazil	$Cl^{-}DR = ae^{-d/t}$	City of Joaõ Pessoa. Ocean Atlantic coast	Wet candle
[27]		$Cl^{-}DR = ad^{-b}$		
[28]	Cuba	$Cl^{-}DR = ae^{-d/t}$ $Cl^{-}DR = ad^{-b}$	North coast of Havana city. Ocean Atlantic coast	Dry Plate
[29]		$Cl^{-}DR = ae^{-d/t}$	Coastal zone west of Havana. Atlantic Ocean	
[30]	Sweden	$Cl^{-}DR = ad^{-b}$	North Sea/Sweden	Weather vane
[31]	South Korea	$Cl^{-}DR = ad^{-b}$	East Sea, West Sea, South Sea	K3-type salinity measurement device
[32]	Australia	$Cl^{-}DR = ae^{-d/8.30} + a_1 e^{-d/18067.6}$	Coastal zone of the Norfolk Island. South Pacific	Rainwater collector

Table 2
Fitted models wherethe influence of *RH* on $Cl^{-}DR$ is demonstrated.

OES (m)	Regressions $Cl^{-}DR = m \pm b[RH] \pm c[T] \pm d[V]$	R^2 (%)	r_{exp}	P (<0.05)
1	$Cl^{-}DR = -355.27 + 1.27(RH)$	40	0.62	0.04
2	$Cl^{-}DR = -122.42 + 1.72(RH)$	50	0.71	0.01
3	$Cl^{-}DR = -121.23 + 1.69(RH)$	51	0.74	0.008
4	$Cl^{-}DR = -123.91 + 1.70(RH)$	63	0.81	0.002
5	$Cl^{-}DR = -137.51 + 1.85(RH)$	73	0.86	0.0005
6	$Cl^{-}DR = -105.28 + 1.48(RH)$	79	0.89	0.0002
7	$Cl^{-}DR = -106.21 + 1.56(RH)$	81	0.9	0.0001
Average	$Cl^{-}DR = -177.20 + 1.43(RH)$	77	0.8	0.0005

critical values (r_c) for a significance level of $P < 0.05$, it was found that $r_{exp} > r_c$, validating the model's description of $Cl^{-}DR$ reduction as *RH* increases. These findings may influence our understanding of the kinetics behind the electrochemical atmospheric corrosion of carbon steel. Interestingly, in two high-potential construction zones in Cuba and Manabí, increases in *RH* coupled with temperature variations were associated with $Cl^{-}DR$ increases. This phenomenon was observed in specific coastal zones between Bahía de Caráquez-San Vicente and the Manta port zones, leading to the categorization of atmospheric corrosivity levels as High (C4) and Very High (C5) for carbon steel.

The critical threshold for monthly average *V* above which $Cl^{-}DR$ increased was also evaluated, drawing on global atmospheric corrosion studies and devices for $Cl^{-}DR$ determination (Table 3). Through analysis of annual average $Cl^{-}DR$and monthly average *V* values, a significant relationship was established (Fig. 4). A notable increase in $Cl^{-}DR$ was observed at a monthly average wind speed threshold of 2.3 m s^{-1}, aligning with findings from the coastal zone of the Manta canton and the Baltic Sea in Poland. This suggests that the critical threshold values of *V* in Ecuador are among the lowest worldwide. Moreover, within the wind speed range of 2.3 m $s^{-1}$to 3.4 m s^{-1}, corresponding to light and gentle breezes, a very high $Cl^{-}DR$ was recorded.

These results underscore the aggressive nature of the coastal atmospheric environment in the studied zones, providing critical insights for evaluating durability and planning construction activities. The observed high atmospheric corrosivity categories indicate potential risks for carbon steel structures in these areas.

According to study carried out in Cuba, atmospheric corrosion of AISI-1020 carbon steel, similar to that used in this research study, was assessment in a very aggressive north coast area of Havana. Corrosivity category of the atmosphere was classified as very high (C5) using three ways of assessment. Recently the works to be published are in process of drafting.

Table 3
Critical threshold of the monthly average of *V* above which the $Cl^{-}DR$ increased in atmospheric corrosion studies carried out worldwide.

References	Countries	Threshold *V* ($m\ s^{-1}$)	Coastalstudyzone	Devices
[12]	Ecuador	1.2–1.7	Coastal zone between the cantons of Sucre and San Vicente. PacificOcean.	DryCloth
[13]		2.3	Coastal Zone of the canton of Manta. PacificOcean.	
[32]	Australia	4.8	Coastal zone of the Norfolk Island. South Pacific	Rainwater collector
[34]	Brazil	3.0	Coastal city of Joaõ Pessoa. AtlanticOceancoast.	Wetcandle
[35]	Australia		South coast of Australia. Arctic Ocean Glacier.	
[36]	Spain		South coast of the Mediterranean Sea.	
[37]	Cuba		North coast of	Dry Cloth
In process of drafting		2.6	Havana. Atlantic Ocean.	
[38]	Sweden	5.0	North Sea.	Saltvane
[39]	Russia	6.0	Arctic Ocean Glacier. PacificOcean.	Wetcandle
[40]	Bangladesh	5.5	Coastal city of Chittagong. Indian Ocean.	
[41]	France	5.0	French coast of the Mediterranean Sea.	CollectorFilters
[42]	Poland	2.3	Baltic Sea.	CollectorFilters

3.2. Behavior of monthly average values of r_{corr}-g $m^{-2}$and influential factors

The behavior of monthly average values of r_{corr}-g m^{-2} is depicted in Fig. 5 (a and b). Contrary to expectations, a decrease in corrosion rate with increasing distance from the coastline, analogous to the trend observed for monthly values of $Cl^{-}DR$, is not clearly evident (Fig. 5a).

Elevated monthly average values were recorded from May to August and from October to November 2017 (Fig. 5b), indicating these periods as the most aggressive for atmospheric corrosion in the coastal zone under study. This finding, coupled with consistently high *RH* throughout the year, suggests that both rainy and dry seasons significantly contribute to atmospheric corrosion. Identifying these aggressive

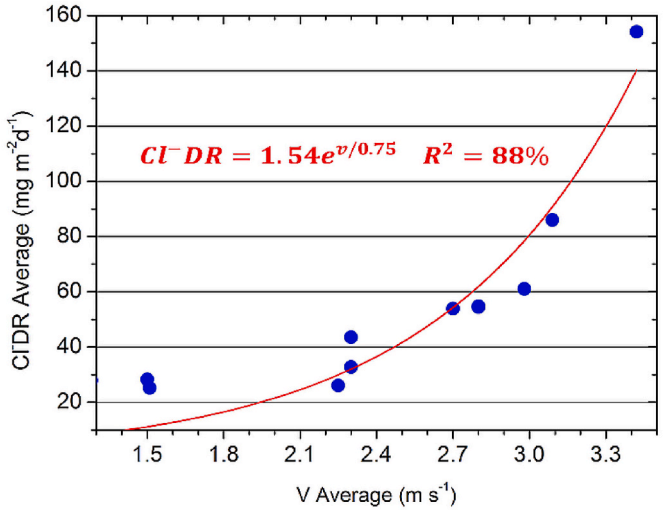

Fig. 4. Influence of *V* on *Cl⁻DR*in the study coastal zone.

periods offers a valuable criterion for the planning of maintenance, repair, and construction activities in coastal zones with high development potential.

Further insights are provided by the analysis of influential factors on the atmospheric corrosion of carbon steel, using a well-fitted statistical model (Table 4). This model illustrates that increases in monthly average values of *RH* and *Cl⁻DR* are associated with increases in the corrosion rate across all OES. The role of *RH* in enhancing the corrosive effect of *Cl⁻DR* facilitating the formation of corrosive saline solutions on steel surfaces is particularly notable. Additionally, the influence of *Cl⁻DR* is more pronounced in stations closer to the coastline, exacerbated by a decrease in average annual temperature (*T*).

The influence of temperature is further highlighted by findings from OES-4, where an increase in temperature suggests a reduced persistence of water films on metal surfaces, potentially leading to lower corrosion rates. This suggests that variations in atmospheric corrosivity for carbon steel can be anticipated based on temperature (*T*) and proximity to the coastline.

The impact of *V* on atmospheric corrosion rates was found to be variable. Increased velocity may enhance the deposition of larger, heavier chloride ion salt particles formed in the wave breaker zone. Conversely, a decrease in velocity could result in the deposition of lighter, smaller salt particles, particularly at stations located further inland or at greater distances from the coastline.

Overall, the application of statistical models to understand the factors influencing atmospheric corrosion of carbon steel and other metals common in construction has been underutilized in engineering studies. This contrasts with the extensive research conducted in Cuba, Mexico, and the coastal zones of Manabí, which has leveraged these models to gain significant insights into corrosion processes in coastal environments [43].

3.3. Corrosivity categories of the atmosphere and predictions

Corrosivity category of the atmosphere for the carbon steel in all OES was assessed from the three annual values of atmospheric corrosion rate (r_{corr}-$g\ m^{-2}y$ *and* $\mu m\ y^{-1}$) calculated. High (C4) corrosivity category of the atmosphere for the carbon steel was determined in the OES-1 placed from the wave breaker zone (coastline) towards the interior of the sea. A medium (C3) corrosivity category of the atmospherefrom OES-2 to OES-7 was determined (Table 5).

The zone where the building works of the structures could be carrying out. Classification intervals of the r_{corr}-$g\ m^{-2}y$ *and* $\mu m\ y^{-1}$ are established in the atmospheric corrosion specialty standards, not only for carbon steel, but also for other metallic materials widely used in the building industry (zinc, copper and aluminum). The values for zinc have been used for galvanized steel in atmospheric corrosion studies carried out in Cuba and Mexico [44,45].

According to typical description of the aggressive coastal atmospheric environment in the study zones, higher corrosivity categories of the atmosphere (very high C5, and extreme CX) for the carbon steel were expected. Thus, the *RH* increase influence in the *Cl⁻DR* decrease in saline solution form on kinetics of the electrochemical atmospheric corrosion phenomenon of carbon steel is demonstrated. On the other

Table 4
Fitted models where the influence of*Cl⁻DR, RH, T and V* on $r_{corr}$is demonstrated.

OES (m)	Regressions	R^2 (%)	P (<0.05)
1	$r_{corr} = 211.68 + 0.79(Cl^{-}DR) + 0.59(RH) - 5.97(T) - 7.06(V)$	88	0.0012
2	$r_{corr} = 267.55 + 4.02(Cl^{-}DR) + 2.35(RH) - 1.62(T) + 20.13(V)$	93	0.0002
3	$r_{corr} = 137.95 + 1.84(Cl^{-}DR) + 0.59(RH) - 0.25(T) - 3.36(V)$	86	0.0002
4	$r_{corr} = -62.28 + 3.63(Cl^{-}DR) + 0.45(RH) + 4.25(T) + 7.78(V)$	95	0.0001
5	$r_{corr} = -546.67 + 2.08(Cl^{-}DR) + 4.56(RH) + 4.22(T) + 23.79(V)$	96	0.0000
6	$r_{corr} = -433.76 + 3.26(Cl^{-}DR) + 3.30(RH) + 3.17(T) - 21.66(V)$	97	0.0000
7	$r_{corr} = -529.16 + 4.89(Cl^{-}DR) + 3.23(HR) + 7.99(T) - 18.01(V)$	97	0.0001

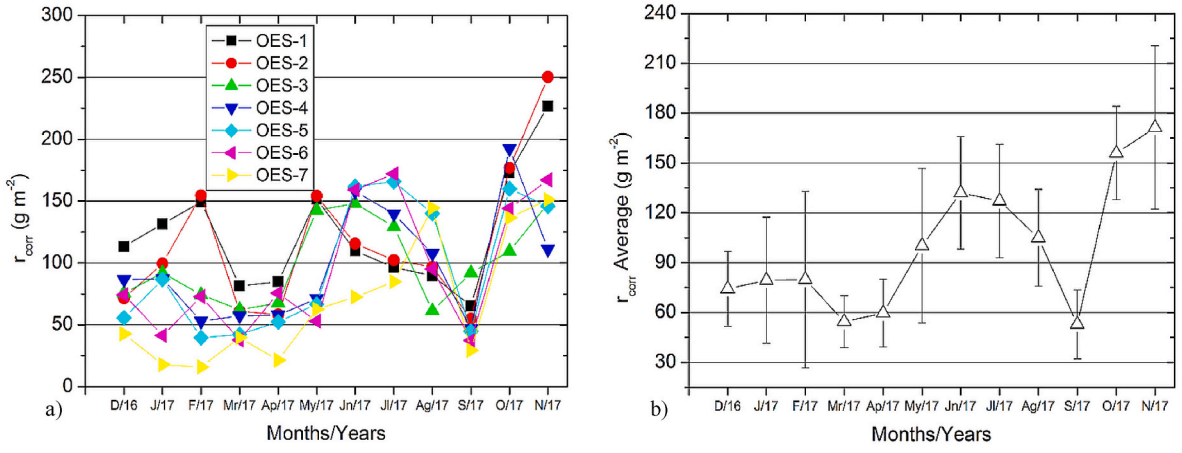

Fig. 5. Behavior of monthly average values of r_{corr}-$g\ m^{-2}$.

Table 5
Corrosivity categories of the atmosphere for the carbon steel determined in all OES.

OES	r_{corr} ($g\ m^{-2}y^{-1}$)	Corrosivity categories of the atmosphere	r_{corr} ($\mu m\ y^{-1}$)	Corrosivity categories of the atmosphere
1	566	C4-High	72.0	C4-High
	565	400 $<r_{corr}\leq$ 650	71.8	50 $<r_{corr}\leq$ 80
	564		71.7	
2	385	C3-Medium	49.0	C3-Medium
	384	200 $<r_{corr}\leq$ 400	48.8	25 $<r_{corr}\leq$ 50
	386		49.1	
3	272	C3-Medium	34.6	C3-Medium
	273	200 $<r_{corr}\leq$ 400	34.7	25 $<r_{corr}\leq$ 50
	271		34.4	
4	259	C3-Medium	32.8	C3-Medium
	262	200 $<r_{corr}\leq$ 400	33.3	25 $<r_{corr}\leq$ 50
	261		33.3	
5	258	C3-Medium	32.8	C3-Medium
	263	200 $<r_{corr}\leq$ 400	33.4	25 $<r_{corr}\leq$ 50
	260		33.0	
6	256	C3-Medium	32.5	C3-Medium
	254	200 $<r_{corr}\leq$ 400	32.3	25 $<r_{corr}\leq$ 50
	257		32.6	
7	255	C3-Medium	32.4	C3-Medium
	258	200 $<r_{corr}\leq$ 400	32.8	25 $<r_{corr}\leq$ 50
	254		32.3	

hand, very high *RH* and $Cl^{-}DR$ could influence a considerable decrease in the solubility of oxygen in the water deposited in the interstices between the layers of oxides formed and on the surface of the of carbon steel specimens. The cathodic reaction of the oxygen will be affected:

$$O_2 + 2H_2O + 4e^{-} \rightarrow 4OH^{-} \quad (6)$$

Hence, structural elements of reinforced concrete and carbon steel subjected to the condition of total immersion in seawater are not affected by corrosion. This is not the case for the tidal and splash exposure conditions where atmospheric corrosion is accelerated [46].

A similar result was obtained in a coastal zone in Spain. The study was carried during six months. Two OES were placed at different distance from the sea. Lower atmospheric corrosion for the same carbon steel was determined where higher $Cl^{-}DR$ values were measured in the OES placed at a higher distance from the coastline. Monthly and annual average *RH* values (84%) were also very high [47]. The explanation was based in the less oxygen solubility in the aqueous layer of precipitated water on the metallic surface with very high chloride concentration. The effect occurred in the coastal zone of Spain as a non-isolated occurrence was demonstrated in other research studies carried out [48,49]. In order to rigorously confirm this effect, is very important to have more information from very severe coastal atmospheres. To continue with carry out of atmospheric corrosion studies in the coastal zone of high construction potential not only in Ecuador but also worldwide is necessary.

Prediction of corrosivity categories of the atmosphere using the model (5) is demonstrated (Fig. 6a and b). According to classification intervals of atmospheric corrosion (*D*-$g\ m^{-2}$ and μm) established in the atmospheric corrosion specialty standard for the carbon steel over the times of exposure, corrosivity categories of the atmosphere determined are kept from two to 20 years in each OES. Due to the values of *D* were calculated from the annual atmospheric corrosion rate experimentally determined at the year of study (r_c-$g\ m^{-2}\ y^{-1}$ and $\mu m\ y^{-1}$), prediction of corrosivity categories of the atmosphere determined can be considered accurate.

Prediction of corrosivity categories of the atmosphere for carbon steel, as well as for the metallic materials most commonly used in the building industry using the model (5), has been demonstrated in the referenced studies carried out in the coastal zones of Manabí, as well as in studies carried out in coastal zone of high construction potential worldwide [50,51]. However, in a large study carried out in Colombia, nonlinear regression models describing the mass loss of carbon steel and galvanized steel as a function of the aggressivity corrosion of the atmosphere were useful for predictions in the short term. Coefficients of determination R^2 were higher than 90% in most cases [52].

To guarantee a long service life for the structures to be built, determination and prediction of corrosivity category of the atmosphere in any coastal zone of high construction potential can be considered as durability requirement.

4. Conclusions

The research conducted on atmospheric corrosion of carbon steel in Port Lopez, located in the coastal zone of Manabí province, Ecuador, yields several pivotal conclusions. This study underscores the significance of understanding the aggressive coastal atmospheric environment's impact on carbon steel, particularly highlighted by the anticipated high corrosivity categories (very high C5 and extreme CX) based on the analysis of monthly average values of meteorological parameters and $Cl^{-}DR$. These expectations stem from the critical influence of meteorological parameters on $Cl^{-}DR$and the proximity to the coastline. Furthermore, the investigation identified a critical threshold for the monthly average values of velocity beyond which $Cl^{-}DR$ notably increases, marking one of the lowest thresholds recorded globally. Interestingly, the study also revealed a medium (C3) corrosivity category for carbon steel positioned inland, suggesting that the extremely high

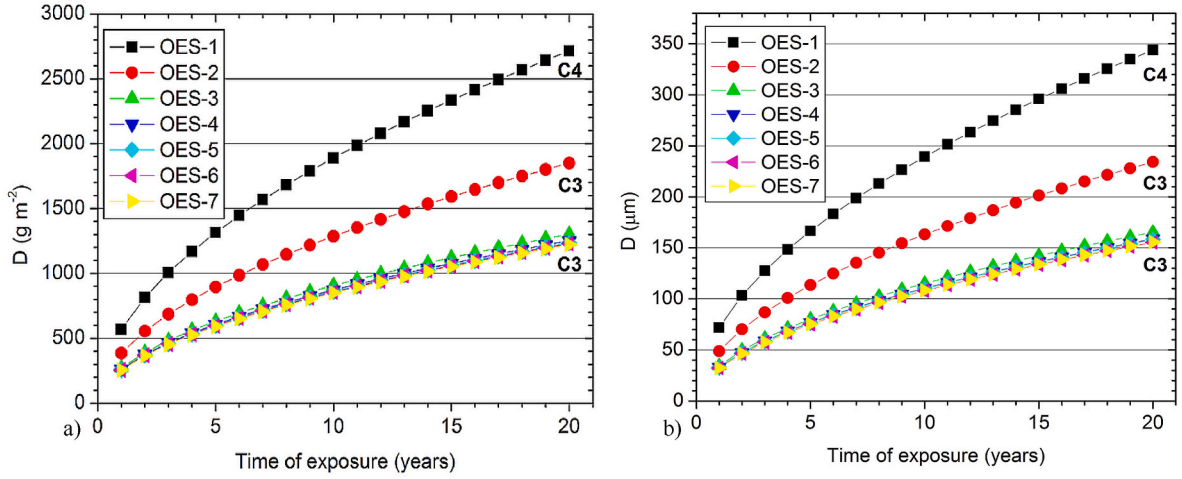

Fig. 6. Prediction of corrosivity categories of the atmosphere for the carbon steel in all OES.

relative humidity characteristic of the study area might play a role in reducing Cl-DR in its saline dissolution form. This elevated RH, coupled with $Cl^{-}DR$, could significantly diminish the solubility of oxygen in water present within oxide layer interstices and on carbon steel surfaces, thereby impacting the cathodic oxygen reaction.

CRediT authorship contribution statement

Juan Carlos Guerra-Mera: Writing – original draft, Resources, Investigation, Formal analysis, Conceptualization. **Ángel Ramón Sabando García:** Visualization, Resources, Methodology, Data curation. **Miriam Goretty Pin -Mera:** Writing – review & editing, Visualization, Validation, Conceptualization. **Joan Manuel Rodríguez-Díaz:** Writing – review & editing, Visualization, Validation, Resources. **Abel Castañeda-Valdés:** Writing – review & editing, Visualization, Validation, Supervision, Formal analysis, Conceptualization.

Declaration of competing interest

The authors declare that they have no known competing financial interests or personal relationships that could have appeared to influence the work reported in this paper.

Data availability

Data will be made available on request.

Acknowledgements

The authors want to express their gratitude to the Faculty of Mathematics, Physics and Chemistry of the Technical University of Manabí for the logistic support provided for the execution of the research study.

References

[1] S. Xianming, et al., Durability of steel reinforced concrete in chloride environments: an overview, Construct. Build. Mater. 30 (2012) 125–138.
[2] O. Trocónis, et al., Duracon Collaboration Durability of concrete structures: DURACON, an Iberoamerican project. Preliminary results, Build. Environ. 4 (7) (2006) 952–962.
[3] Ueli M. Angst, Challenges and opportunities in corrosion of steel in concrete, Mater. Struct. 51 (2018) 1–20.
[4] Bai Zhang, et al., Deteriorationof bond performance between BFRP bars and coral aggregate concrete incorporatingslag-basedgeopolymersunderseawatercorrosionenvironments, Construct. Build. Mater. 411 (2024) 134518.
[5] ISO 9223, Corrosion of Metals and Alloys. Corrosivity of Atmosphere. Classification, Determination and Estimation, 2012.
[6] O. Reinosa, et al., Incidencia de los agentes agresivos de dos regiones típicas de Ciudad de La Habana sobre muestras de gomas experimentales, Rev. CENIC Ciencias Quimicas 38 (3) (2007).
[7] A. Castañeda, et al., Evaluación de sistemas de protección contra la corrosión en la rehabilitación de estructuras construidas en sitios de elevada agresividad corrosiva en Cuba, Rev. Const. Chi 11 (3) (2012) 49–61.
[8] A. Castañeda, et al., Research Project proposal: impact of the aggressive coastal environment of Cuba's atmosphere on the durability of construction-manufacturing materials from China, Rev. CENIC Ciencias Quimicas 54 (2022) 96–108.
[9] M. Morcillo, et al., Looking Back on Contributions in the field of atmospheric corrosion offered by the MICAT ibero-American testing network, Int J Corr 1 (2012) 1–24.
[10] F. Cadena, et al., Corrosión Metálica en Ambientes Exteriores e Interiores en las ciudades de Quito y Esmeraldas, Rev. EPN. 33 (2) (2014).
[11] J.C. Guerra Mera, et al., Estudio preliminar de la agresividad corrosiva de la atmósfera en el puente de los Caras, Manabí, Ecuador, Rev. CENIC Ciencias Quimicas 47 (2016) 17–30.
[12] J.C. Guerra, et al., Atmospheric corrosion of low carbon steel in a coastal zone of Ecuador: anomalous behavior of chloride deposition versus distance from the sea, Rev. Mat. Corr. 69 (10) (2018) 1–16.
[13] J.C. Guerra Mera, et al., Corrosividad de la atmósfera sobre el acero al carbono en una zona costera del cantón de Manta en Manabí, Ecuador, Rev CENIC (Cent. Nac. Investig. Cient.) Cienc. Quim. 54 (2023) 166–183 (publicación continua).
[14] L. Mariaca, et al., Atmospheric corrosion dose/response functions from statistical data analysis for different sites of Mexico, Innov. Corros. Mater. Sci. 4 (2014) 11–20.
[15] ISO 9225, Corrosion of Metals and Alloys - Corrosivity of Atmospheres - Measurement of Pollution, 2012.
[16] ISO 8407, Corrosion of Metals and Alloys — Removal of Corrosion Products from Corrosion Tests Specimens, 2009.
[17] ISO 9226, Corrosion of Metals and Alloys – Determination of Corrosion Rate of Standard Specimen for the Evaluation of Corrosivity, 2012.
[18] ISO 9224, Corrosion of Metals and Alloys. Corrosivity of Atmospheres. Guiding Values for the Corrosivity Categories, 2012.
[19] A. Castañeda, et al., Airborne salinity penetration in the coastal tropical climate of Havana City Cuba, Rev CENIC (Cent. Nac. Investig. Cient.) Cienc. Quim. 46 (2015) 90–99. Número Especial.
[20] G. Meira, et al., Measurement and modelling of marine salt transportation and deposition in a tropical region, Corrosion Sci. 50 (2008) 2724–2731.
[21] F. Corvo, et al., Outdoor-Indoor corrosion of metals in tropical coastalatmospheres, Corrosion Sci. 50 (2008) 220–230.
[22] F. Corvo, et al., "Corrosion ResearchFrontiers. Atmospheric Corrosion in Tropical Climate. On the Concept of Wetness and its Interaction with Contaminants Deposition. Electroanalytical Chemistry: New Research, Nova Science Publishers, New York, EE.UU. 2008 *(Chapter 2)*.
[23] D.Y. Fernández Soto, et al., Estudio de la corrosión atmosférica en el Puerto del Mariel, Rev CENIC (Cent. Nac. Investig. Cient.) Cienc. Quim. 46 (2015) 47–58. Número Especial.
[24] A. Castañeda, et al., Estudio de la corrosión atmosférica en una zona estratégica de Cuba, Rev CENIC (Cent. Nac. Investig. Cient.) Cienc. Quim. 46 (2015) 47–58. Número Especial.
[25] J. Alcantara, et al., Airborne chloridedeposit and itseffecton marine atmosphericcorrosion of mildsteel, Corrosion Sci. 97 (2015) 74–88.
[26] G.R. Meira, et al., Efecto de la distancia al mar en la agresividad por cloruros en estructuras de hormigón en la costa brasileña, Rev. Mater. Const. (2003). Vol271 - 272, pp. 175 – 18.
[27] G.R. Meira, et al., Measurement and modelling of marine salt transportation and deposition in a tropical region in Brazil, Rev. Atmosph. Env. 40 (2006), 5596–560.
[28] A. Castañeda, et al., Penetration of marine aerosol in a tropical coastal City: havana, Rev. Atm.UNAM. 31 (2018) 87–104.
[29] A. Castañeda, et al., Outdoor-indoor atmospheric corrosion in a coastal wind farm located in a tropical island, Rev. Eng. Jr. 21 (2) (2016) 44–62.
[30] E.R. Gustafsson, et al., Island transport of marine aerosol in southern Sweden, Rev. Atmosph. Env. 34 (2000) 313–325.
[31] J. Lee, et al., Salinity and distributions on seashore concrete structure en Korea, Build. Environ. 41 (2006) 1447–1453.
[32] P. Campos, et al., Spatio-temporal distribution of atmospheric chloridedeposition over a small island, Hydrol. Proced. 15052 (2023) 1–17.
[33] A. Castañeda, et al., The service life of reinforced concrete structures in an extremely aggressive coastal city. Infuence in concrete quality, Mater. Struct. 56 (12) (2023) 2–17.
[34] G.R. Meira, et al., Modelling sea-salt transport and deposition in marine atmosphere zone –A tool for corrosion studies, Corros.Sci. 50 (2008), 2724-273.
[35] I.S. Cole, et al., Holistic model for atmospheric corrosion.Part II–Experimental measurements of deposition of marine salts in a number of long range studies, Corrosion Eng. Sci. Technol. 38 (2003) 259–266.
[36] S. Feliu, et al., Effect of distance from sea on atmospheric corrosion rate, Rev. Corr. NACE 55 (1999) 883–891.
[37] A. Castañeda, et al., Airborne salinity penetration in the coastal tropical climate of Havana City Cuba, Rev CENIC (Cent. Nac. Investig. Cient.) Cienc. Quim. 46 (2015) 90–99. Número Especial.
[38] E.R. Gustafsson, et al., Dry deposition and concentration of marine aerosols in a coastal area, Sweden, Atmos. Environ. 30 (1996) 977–989.
[39] P.V. Strekalov, et al., Atmospheric corrosion of electroplates in sea climate: protective decorative functions and service life of plate, Rev. Prot. Met 37 (2000) 176–196.
[40] M. Khandaker, et al., Evaluation of the effect of marine salts on urban built infrastructure, Build. Environ. 44 (2009) 713–722.
[41] J. Piazzola, et al., Contribution of marine aerosols in the particle size distributions observed in Mediterranean coastal zone, Atmos. Environ. 31 (1997) 2991–3009.
[42] T. Petelski, et al., Sea salt emission from the coastal zone, Ocean 42 (2000) 399–410.
[43] F. Corvo, et al., Atmospheric corrosion in tropical humid climates.Environmental degradation of infrastructure and cultural heritage in coastal tropicalclimate, Transworld Research Network 37/661 (2) (2009). Fort P.O., Trivandrum-695 023, Kerala, India.
[44] A. Castañeda, et al., Atmospheric corrosion study in a Harbor located in a tropical island, Rev. Mat. Corr. 69 (10) (2018) 1472–1744.
[45] E. Meraz, et al., Etapas iniciales del zinc runoffen clima tropical húmedo, Rev. Métall. 43 (No.2) (2007) 85–100.
[46] M.N. Haque, et al., A prelude to designing durable concrete structures in the Arabian Gulf, Build. Environ. 42 (2007) 2410–2416.
[47] M. Morcillo, et al., Atmospheric corrosion of mild steel in chloride-richenvironments. Questionsto be answered, Mater. Corros. 66 (2015) 882–892.
[48] L. Espada, et al., Estudio de la velocidad de corrosión de aceros de bajo contenido de carbono en nieblas salinas de distinta concentración, Rev. Iberoam. Corros. Prot XIX (1988) 227–238.
[49] R. Pascual, et al., Influencia de la concentración de ion cloruro sobre la corrosión atmosférica de un acero al carbono bajo capa de fase de humedad, Rev. Iberoam. Corros. Prot XIX (1988) 227–238.

[50] Y.M. Panchenko, et al., Long-term prediction of metal corrosion losses in atmosphere using a power-linear function, Corrosion Sci. 109 (2016) 217–229.
[51] Y.M. Panchenko, et al., Long-term forecast of corrosion mass losses of technically important metals in various world regions using a power function, Corrosion Sci. 50 (2014) 3446–3454.
[52] E. Velilla, Modelos de pérdida de masa de acero por corrosión atmosférica en Colombia usando inteligencia computacional, Rev. Fac. Ing. Univ. Antioquia 49 (2009) 81–87.